INSTITUTE OF PLASMA PHYSICS

NAGOYA UNIVERSITY

# RESEARCH REPORT

NAGOYA, JAPAN

# A Scaling Law for High Density Tokamaks and Its Application to J.I.P.P. T-II Device

Sanae INOUE*, Kimitaka ITOH*
and
Yoshinosuke TERASHIMA

IPPJ-318 December 1977

Further communication about this report is to be sent to the Research Information Center, Institute of Plasma Physics, Nagoya University, Nagoya 464, Japan.

---

*Permanent address: Department of Physics, University of Tokyo

Abstract

A scaling law for high density and high current tokamaks is presented on the basis of the non-local theory of drift instability of current-carrying plasma with the assumption of quasi-linear saturation level. It is shown that the energy confinement time scales as $\tau_E \propto nq/\sqrt{T}$ (n and T are the averaged density and temperature) due to the pure current-driven mode in the relatively lower density region and $\tau_E \propto B/\sqrt{n}$ (B is the toroidal magnetic field) due to the usual collisional drift instability in the higher density region. The effects of the trapped particles are assumed to be negligible.

A test-experiment of the scaling law on the J.I.P.P. T-II device where both the tokamak operation and the operation with the superposition of helical fields are possible, is proposed.

## 1. Introduction

The purpose of this paper is to present a scaling law for tokamaks based upon the nonlocal theory of drift instability of current-carrying plasma with temperature inhomogeneities.[1] The scaling law is derived from the anomalous transport coefficients of high density plasmas. A second purpose of the paper is to propose a test-experiment of the scaling law on the J.I.P.P. T-II device[2] where both the tokamak operation and the operation with the superposition of helical fields are possible.

The importance of the current-driven drift instability on anomalous transport in toroidal plasmas has been discussed by several authors.[3-6] The previous works are either limited to the local theory, or not inclusive for destabilizing or stabilizing effects of many factors such as rotational transform, magnetic shear, and temperature and density gradients. Coppi et al[3] have shown that the current-driven drift mode contributes appreciably to the heat transport in the Alcator experiment. Their treatment is, however, the local theory where the parallel wave length is arbitrarily chosen and the effect of the shear is not correctly incorporated, although both the plasma current and the presence of the trapped electrons are considered.

In the present analysis we consider the non-local modes of current-driven and collisional drift instabilities in a sheared magnetic field, including the electron and ion temperature gradients. The electro-static approximation is made because electromagnetic perturbations do not give appreciable contribution

to plasma transport.[7] The effect of the trapped particles is neglected, since we are concerned with the scaling law for high density plasmas.

For the estimation of the diffusion coefficient, we use the familiar relation

$$D = \sum_k \left| \frac{\tilde{n}_k}{n_0} \right|^2 \frac{\gamma_k}{\kappa^2} \quad , \qquad (1)$$

with an appropriate assumption for $|\tilde{n}_k/n_0|^2$, where $\kappa$ is the density gradient and $\tilde{n}_k$ is the perturbed density with the wave number k ($n_0$=background density). The growth rate $\gamma_k$ is estimated by the non-local theory. For heat conductivity, we use a similar relation. The summation over the wave number k will be carried out comparing the localization width of unstable mode in the direction of the density gradient with the distance between adjacent rational surfaces. The scaling law is derived from these transport coefficients, which is applicable to high density tokamaks. Firstly, it is expressed in terms of the plasma parameters averaged over the plasma cross section. Secondly, the effects of the radial profiles of the plasma parameters on the scaling law are discussed.

Numerical examples are given for the J.I.P.P. T-II device. Implication of the scaling law to the experimental conditions are discussed. It is shown, for example, that the gross confinement time becomes longer as the helical magnetic field increases for the fixed value of the total transform angle which is the sum of the contributions from the helical field and the plasma current. An experiment to confirm such a

tendency is proposed.

In Sec.2, the anomalous transport coefficients are presented. In Sec.3, the scaling law is expressed in terms of the averaged quantities of the plasma parameters and its numerical value is estimated for the J.I.P.P. T-II device. In Sec.4, the effects of radial profiles of the plasma parameters are examined. In Sec.5, the experimental procedures in J.I.P.P. T-II are discussed. In Sec.6, the conclusions are presented.

## 2. Anomalous Transport Coefficients

We here discuss some characteristics of the current-driven or collisional drift instability. The geometry we firstly use is a slab with a sheared magnetic field, where the x-axis is taken in the direction of the density gradient (Fig.1). The shear parameter is taken to be $1/\kappa L_s$. The normal mode in the presence of both the plasma current and the electron collisions is obtained in the reference [13]. For the anomalous diffusion coefficient D given in eq.(1), we assume the quasi-linear saturation level

$$\left|\frac{\tilde{n}_k}{n_0}\right|^2 = \frac{\kappa^2}{k_\perp^2} = \frac{\kappa^2}{k^2 + k_x^2} \quad , \tag{2}$$

where we simply write the wave number in the y direction as k, and $k_x^2$ is estimated to be $\mu/\tilde{\rho}_i^2$ (see the Appendix). We now use the following notations; $\nu_e$ is the collision frquency for the electrons, $\rho_i$ the ion Larmor radius, $\rho_i^2 = T_i/m_i\Omega_i^2$,

$\mu=(1/\tau\kappa_e L_s)\sqrt{-\Lambda'/\Lambda}(1+\tau-\tau\Lambda)$, $\tau = T_e/T_i$, $\Lambda = I_0(b)e^{-b}$, $b = k^2\rho_i^2$, $\tilde{\rho}_i^2 = -\Lambda'\rho_i^2$. By adopting the proper eigenmode, we get rid of the ambiguities in the evaluation of $k_{\parallel}$ and $k_x$, which remain to be arbitrary constants in the local approximation. Although the relation (2) was conjectured in the earlier works, it is not yet demonstrated reliably. We may add the following remarks. The recent works[8-10] on nonlinear transport have shown that the quasi-linear saturation, or the saturation due to the density flattening is important and suggested the above relation. Moreover, it means the condition that the cross-field velocity due to the perturbed electric field is equal to the original diamagnetic velocity in magnitude.

These results can directly be used for a plasma column. In this case, k is replaced by m/r where m is an integer, and r is the radius of the concerned rational surface. In the summation, k=m/r takes not all the values (m=1,2,3$\cdots$ ). In the neighbourhood of one rational surface at $r=r_s$, there exist only the (m, n) modes which satisfy $|m/n-q|<q'\delta$ where $\delta$ is the wave localization length. We simply approximate the summation $\Sigma_k$ by the integral $(r/\rho_i)\int d(k\rho_i)$, although this is an overestimation. Hence, we get

$$D = \frac{r\rho_i}{2}\,\omega_{*max}\int\frac{(\gamma/\omega_*)}{b-\mu/\Lambda'}\,db \quad , \tag{3}$$

where $\omega_*=k\kappa T_e/eB$ and the maximum drift frequency is defined by $\omega_{*max}=\kappa T_e/eB\rho_i$. For the growth rate $\gamma$, we substitute the following value of the normal eigenmode which is derived in the Appendix[13], assuming that the contribution of trapped

particle is unimportant. $\gamma$ is expressed as

$$\frac{\gamma}{\omega_*} = \frac{(\omega\tau+\omega_*)^2}{2(1+\tau)\omega_*^2}\left[d_0 + \sqrt{(d_0+2\mu)^2+4d_1^2\left(\frac{u}{v_e}\right)^2-4\mu}\right] , \qquad (4)$$

with

$$\begin{aligned} d_0 &= \frac{\omega_*-\omega}{\omega\tau+\omega_*}\left(\sqrt{\frac{\nu_e}{\omega}}\,\frac{\varepsilon}{\sqrt{2\pi}} + \varepsilon\ell n\,\frac{\sqrt{2}}{\varepsilon}\right) , \\ d_1 &= \frac{\omega_*}{\omega\tau+\omega_*} , \\ \omega &= \Lambda\omega_*/(1+\tau-\tau\Lambda) , \\ \varepsilon &= \sqrt{\frac{m_e}{m_i}\kappa L_s}\left(\frac{\Lambda}{-\Lambda'}\right)^{1/4}\left(\frac{\Lambda}{1+\tau-\tau\Lambda}\right)^{1/2} , \end{aligned} \qquad (5)$$

where u is the electron velocity which supports the plasma current and $v_e=(T_e/m_e)^{1/2}$. It should be noted that $d_0$ is contributed by the electron dissipation and ion gyroradius effect, $d_1$ is due to the current-driven mode, $\mu$ indicates the rate of the convective damping due to the magnetic shear, and $\varepsilon$ is the expansion parameter defined by $\varepsilon \equiv \sqrt{\mu}\,\omega\, L_s/k\,\tilde{\rho}_i\, v_e$ (which is of the order of $\sqrt{\kappa\, L_s\, m_e/m_i}$). We have retained only the terms to the lowest order in $\varepsilon$. As expected, the above expression does not include $k_{\parallel}$. Substituting the current experimental data of tokamaks, we find that the magnitude of the magnetic shear is insufficient for the suppression of the drift wave instabilities. Following the usual way, $\chi$ is approximately evaluated as 2D.

When the current density is high, i.e., $d_1\,\frac{u}{v_e} >> d_0$, we obtain the diffusion coefficient

$$D_{CD} \simeq \frac{\kappa r}{2} \frac{T_e}{eB} \frac{u}{v_e} F_{CD} \quad . \tag{6}$$

The numerical coefficient $F_{CD}$ is a slowly varying function of $\kappa L_s$. The typical value of $F_{CD}$ is tabulated in Table 1. On the other hand, when the density becomes high enough, i.e., $d_0 << d_1 \frac{u}{v_e}$, we obtain

$$\frac{\gamma}{\omega_*} \simeq \frac{(\omega_* \tau + \omega)(\omega_* - \omega)}{(1 + \tau)\omega_*^2} \left( \sqrt{\frac{\nu_e}{\omega}} \frac{\varepsilon}{\sqrt{2\pi}} + \varepsilon \ell n \frac{\sqrt{2}}{\varepsilon} \right) . \tag{7}$$

The diffusion coefficient due to the collisional drift instaibility is thus found to be

$$D_{CM} \simeq \frac{\kappa r T_e}{eB} \sqrt{\frac{m_e}{2\pi m_i} \frac{\nu_e}{\omega_{*max}} \kappa L_s} \; F_{CM} \quad . \tag{8}$$

The typical value of the numerical coefficient $F_{CM}$ is also shown in Table 1. Note that this result differs from the previous ones.[11] Equations (6) and (8) show the diffusion coefficient in the two limits.

When the plasma temperature is high and the density is low enough, the above results are to be compared with the transport coefficients due to the dissipative trapped electron mode

$$\begin{aligned} D_{TE} &\simeq \left(\frac{a}{R}\right)^{3/2} \frac{3}{\nu_e} \frac{\eta_e}{r_n} \left(\frac{T_e}{eB}\right)^2 , \\ \chi_{TE} &\simeq \left(\frac{a}{R}\right)^{2/3} \frac{15\eta_e}{\nu_e r_n^2} \left(\frac{T_e}{eB}\right)^2 , \end{aligned} \tag{9}$$

where $\eta_e = \nabla \ell n T_e / \nabla \ell n \; n_0$ and $r_n^{-1} = |\nabla \ell n \; n_0|$. The dissipative trapped electron mode becomes dominant for the condition that

$\nu_e R/r \ll \omega_b = 2(r/R)^{1/2} v_e/qR$ where $\omega_b$ is the bounce frequency of the trapped electrons. In the intermediate regime of $\nu_e R/r \gtrsim \omega_b$, the current-driven mode and the dissipatve trapped electron mode coexist,[3] and their combined effect will govern the plasma confinement.

## 3. Scaling Law and Its Application to J.I.P.P. T-II Device

Scaling law for high density tokamaks is deduced from the results obtained in the preceding section as follows. The energy confinement time $\tau_E$ is evaluated by $a^2/\chi = a^2/2D$. Calculating the numerical constants included in eqs.(6) and (8), we get the diffusion coefficients both in the current-driven (CD) regime and the collisional mode (CM) regime as

$$D_{CD} \simeq 15.2 \sqrt{\bar{T}}/\bar{n}qR \quad (m^2/sec) \ ,$$
$$D_{CM} \simeq 0.4 \sqrt{\kappa L_s \bar{n} a} \ /B \quad (m^2/sec) \ , \tag{10}$$

where $\bar{T}$ (averaged temperature) $\bar{n}$ (averaged density), R major radius, a minor radius, B are measured in units of keV, $10^{13}$/cc, m, cm, and 10 kG, respectively. In the above, we have evaluated the averaged value of $\kappa r$ as 1/4. Then the energy confinement time is given by

$$\tau_E \simeq 3 \times 10^{-3} \bar{n}qRa^2 / \sqrt{\bar{T}} \quad (msec), \quad \text{for CD regime,}$$
$$\tau_E \simeq 0.12 \ a^2 B / \sqrt{\bar{n} a \kappa \ L_s} \quad (msec), \quad \text{for CM regime.} \tag{11}$$

We apply this formula to the plasma confinement in the J.I.P.P. T-II device. The machine parameters and the typical plasma parameters are listed in Table 2. It should be noted that the magnetic shear is not sufficient to stabilize the drift wave instabilities. The possible modes to limit the plasma confinement are the collisional mode (CM), current-driven mode (CD), and the dissipative trapped electron mode (TE). When the plasma density is low, CD and TE modes become unstable and the resultant diffusion is inversely proportional to $\bar{n}$. The scaling due to the CD mode and that due to the TE mode show a similar $\bar{n}$ dependence, however, their temperature dependences are far different. As will be shown in the next section, the TE mode does not play an important role in the experimental regime in Table 2. We set our scope on the current-driven mode and the collisional mode in the following.

Using eqs.(10) and (11), we have the diffusion coeffiecint for both the current driven regime and the collisional regime as

$$D_{CD} \simeq 3.5/\bar{n} \simeq 16.7\sqrt{\bar{T}}/\bar{n}q \qquad (m^2/sec),$$

$$D_{CM} \simeq 0.63\sqrt{\bar{n}}/B \qquad (m^2/sec),$$

where $\bar{n}$, T, B are measured in units of $10^{13}$/cc, keV and 10 kG respectively. The energy confinement time is

$$\tau_E \simeq 0.7\,\bar{n}\,q\,/\!/\sqrt{\bar{T}} \qquad (msec) \qquad \text{for CD regime},$$

$$\tau_E \simeq 8\,\frac{B}{\sqrt{\bar{n}}} \qquad (msec) \qquad \text{for CM regime}.$$

This result is illustrated in Fig.2. The transition from the current-driven regime to the collisional regime occurs around $\bar{n} = \bar{n}_c \simeq 4 \times 10^{13}$/cc, where the maximum confinement time is expected approximately 10 msec. The electron temperature scales for the total plasma current I and the safety factor on the surface q as

$$\bar{T} \propto I^{\frac{2}{3}} q^{\frac{1}{3}} \qquad \text{in CD mode regime} \quad (\bar{n} < \bar{n}_c) \ ,$$

$$\bar{T} \propto \bar{n}^{-\frac{3}{5}} I^{\frac{6}{5}} q^{\frac{2}{5}} \quad \text{in CM mode regime} \quad (\bar{n} > \bar{n}_c) \ .$$

Note also that the density at the transition point, $n_c$, scales as

$$\bar{n}_c \propto I^{2/3} \bar{T}^{1/3}$$

In real plasmas the plasma parameters have radial profiles, and the transport coefficient has also radial dependence. One will see such a situation that in the central core of the plasma column the current-driven mode dominates and, at the same time, in the outer edge of the plasma the collisional mode dominates. This may make the transition between CD mode and CM mode somewhat vague. The analysis which takes the parameter distribution into consideration will be given in the next section.

Table 1

| $\kappa L_s$ | 10 | |
|---|---|---|
| $\tau$ | 1 | 3 |
| $F_{CD}$ | 1.72 | 1.82 |
| $F_{CM}$ | 0.34 | 0.42 |

Table 2

| | |
|---|---|
| $B_t$ | 30 kG |
| a | 17 cm |
| R | 91 cm |
| $I_p$ | 100 kA |
| $\bar{n}$ | $(1\text{-}5) \times 10^{13}$/cc |
| $T_{eo}$ | 1 keV |
| $T_i/T_e$ | 0.4-0.8 |
| $\bar{u}/v_e$ | $(1.7\text{-}8.4) \times 10^{-2}$ |
| $Z_{eff}$ | 2 |

## 4. Consideration of Radial Profiles

To analyze the scaling law more precisely, we consider the case where n, $T_e$, J are assumed to be the gaussian distributions as shown in Table 3. The radial dependences of the other quantities are also shown in Table 3. The numerical values are referred to the typical experimental conditions of J.I.P.P. T-II. As shown in the Appendix, the current-driven (CD) mode becomes unstable even in the presense of the fairly steep electron temperature gradient and the ion temperature gradient promotes it, so that the CD mode may not be stabilized unless the shear is strong enough. Keeping these facts in mind , we show the radial profiles of the ratio of the electron drifting velocity to its thermal speed, $u/v_e$(instability source indicated by solid lines) and the shear strength ($1/\kappa L_s$, indicated by the dashed line) for the case of $\eta_e$=2 and 4/3 (for the fixed total plasma current) in Fig.3, from which we find that the shear is insufficient to stabilize the CD mode near the center of the plasma column even when $\eta_e$=2.

We estimate the radial distribution of the transport coefficient by using eqs.(3) and (4). The result is shown in Fig.4 for the various values of the plasma density. We show the density dependence of the diffusion coefficient, D(n), for the various points in the radial direction in Fig.5. One sees that the density dependence of the diffusion coefficient is very similar to that obtained in the preceding section. Hence the coefficients expressed in the averaged quantities are of good approximation for the arguments of the overall plasma

confinement time.

For the plasma parameters of J.I.P.P. T-II, one may expect that the plasma may suffer from the trapped particle instabilities. However, the dissipative trapped electron mode (TE) does not appear unless the operating plasma has lower density or higher temperature ($\bar{n} < 10^{13}$/cc, or $T_e > 1$ keV). We confirm this by calculating the bounce frequency and the effective collision frequency of the trapped electrons as functions of the radius. In Fig.6, we show schematically the instability criteria in the plasma column as a function of the averaged plasma density. The dotted lines show the condition of $\nu_{eff}/\omega_b=1$ which means that the deeply trapped particles become barely free from collisions. The solid lines show the condition $\nu_{eff}/\omega_b=0.5$. Only in the shaded portions divided by the solid line, the TE mode may appear, since the TE mode is induced by the trapped electrons. Therefore, in high density regime, it is not necessary to consider the contribution of trapped electrons to the transport coefficients.

We also show in Fig.6 the lines which satisfy the condition $u/v_e = 1/\kappa L_s$ for $\eta_e = 2$, 4/3(chained lines). One sees that in the inner part of the plasma column divided by these lines for each $\eta_e$, the CD mode cannot be stabilized by the shear.

The above results are based upon the gaussian distributions. Almost the same results apart from the numerical factors of the order of unity are obtained for the other configuration such that $n=n_0(1 - x^2)$, $T_e = T_{e0}(1-x^2)^{3/2}$. It is therefore concluded that the transpart coefficients taking account of the radial

profiles of the plasma parameters coincide well with those obtained with the averaged plasma parameters.

Table 3

| (parameters) | (radial distributions, $x \equiv r/a$) |
|---|---|
| $n$ | $n_0 \exp(-\frac{3}{2}x^2)$, $\bar{n}=0.52\, n_0$ |
| $\kappa$ | $3x/a$ |
| $T_e$ | $T_{eo} \exp(-\frac{3}{2}\eta_e x^2)$ |
| $J$(current density) | $1.05(J_0/q_0)\exp(-\frac{9}{4}\eta_e x^2)$ |
| $q_0 \equiv q(r=0)$ | $2.12/\eta_e(1-\exp(-\frac{9}{4}\eta_e))$ |
| $q$ | $q_0 \frac{9}{4}\eta_e x^2/(1-\exp(-\frac{9}{4}\eta_e x^2))$ |
| $q(r=a)$ | 4.77 |
| $u/v_e$ | $(0.064/q_0)\exp[-\frac{3}{2}x^2(\eta_e-1)]$ |
| $\nu_e$ | $2.16\cdot10^5(Z_{eff}/2)\exp[(\frac{9}{4}\eta_e-\frac{3}{2})x^2]$ |
| $\nu_{eff}$ | $5.78\cdot10^5 Z_{eff}\, x^{-1}\exp[(\frac{9}{4}\eta_e-\frac{3}{2})x^2]$ |
| $\omega_b$ | $1.18\cdot10^7 x^{1/2}\exp(-\frac{3}{4}\eta_e x^2)[1-\exp(-\frac{9}{4}\eta_e x^2)]$ $\cdot(9\eta_e x^2/4)^{-1}$ |
| $\omega_{*max}=\frac{\kappa T_e}{eB}\frac{1}{\rho_i}$ | $8.82\cdot10^6 x \exp(-\frac{3}{4}\eta_e x^2)$ |

## 5. A Test Experiment in J.I.P.P. T-II Device with Helical Fields

Based upon the scaling law both in the cureent-driven (CD) regime and the collisional drift (CM) regime, we would like to propose a test experiment on the shear effect, controlling the rotational transform and the shear by use of the external helical windings. We first consider the case that the toroidal field ($B_t$) and the total rotational transform $\iota = \iota_0 + \iota_H$ are fixed (the procedure 1). In this case, the confinement time $\tau_c$ will change as

$$\tau_c = \tau_0 \left(\frac{\iota}{\iota - \iota_H}\right)^{7/6} \qquad \text{for CD mode,}$$

$$\tau_c = \tau_0 \qquad \text{for CM mode,}$$

where $\tau_0$ stands for the confinement time obtained by tokamak operation. The confinement time $\tau_c$ increases appreciably (about 1,6 $\tau_0$) when one third of the total value of the rotational transform is made by the external windings ($\iota_H = \iota/3$). The temperature changes under this condition as,

$$T = T_0 \left(\frac{\iota - \iota_H}{\iota}\right)^{1/3} \qquad \text{(CD Mode)}$$

$$T = T_0 \left(\frac{\iota - \iota_H}{\iota}\right)^{4/5} \qquad \text{(CM Mode)}$$

where $T_0$ is the value obtained in tokamak operation. The resultant decrease of the temperature is caused by the reduction of the ohmic heating.

For the operation where the plasma current is kept

constant and thus $T_e$ changes little (the procedure 2), the rotational transform angle changes for both the modes from $\iota_T$ to

$$\iota = \iota_H + \iota_T$$

where $\iota_T$ is the value in tokamak operation. In this case, the confinement time remains unaltered provided that the shear parameter and $B_T$ are unchanged.

$$\tau_c = \tau_0 \qquad \text{(for CD and CM regime)}$$

These two procedures illustrate two typical checks to find the way to make use of the freedom introduced by the helical windings. In the procedure 1, $\iota$ is expected to be unaltered. This means that the MHD properties of the gross equilibrium are not so much affected while the diffusion coefficient is reduced (or enhanced) by use of the helical windings. In the procedure 2, it is shown that the expected transport (also the plasma temperature ) remains unaltered, while the rotational transform can be controlled to find the best stability window[12] and the equilibrium with high $\beta$ value. These two typical procedures are illustrated in Fig.7. The above considerations seem to be too idealized. We presuppose that other transport processes such as the radiation loss do not change appreciably in both the procedures, and the stability window is wide. Moreover, we presume that the confined plasma is free from the tearing mode which strongly depends on the current distribution.

## 6 Conclusions

We summarize our conclusions in the followings.

In high density and high current tokamaks, the current-driven drift instability is responsible for the transport, which tends to the standard collisional drift instability in the sufficiently high density region.

The scaling law is deduced from the anomalous transport coefficients based upon the non-local theory and some arguments of non-linear dynamics. The limiting cases of the scaling law is as follows. The energy confinement time scales as $\tau_E \propto nq/\sqrt{T}$ due to the pure current-driven mode in the relatively lower density region and $\tau_E \propto B/\sqrt{n}$ due to the standard collisional drift instability in the higher density region.

Numerical examples of the transport coefficients are given for the J.I.P.P. T-II device. The present experimental conditions correspond to the case where the above scaling law can be applied.

The radial dependences of the transport coefficients are discussed by assuming both the types of radial distribution for the plasma parameters, gaussian and algebraic. The scaling law referred to the averaged parameters is thus found to be adequate for the arguments of the gross confinement time. The radial distribution of the perturbed density or potential can be calculated; its amplitude increases as the plasma radius increases. The inclusion of the temperature gradient enhances the pressure perturbation as shown in eq.(A-10).

For the operation by use of the helical windings in

J.I.P.P. T-II, two typical procedures are proposed. In the first procedure where one lets the helical magnetic field increase keeping the total transform angle constant, the energy confinement time is expected to becomes longer, while MHD activities are not so much affected, provided that this procedure is along the stability window. In the second procedure of keeping the plasma current constant, MHD activities under almost the same transport coefficients will be studied. The validity of the present model will be tested by these procedures.

For detailed comparisons of the present model with the experimental results (which are not enough at present), a computer work is required. Further study on the basis of our treatment is also necessary.

## References


1) S.Inoue, K.Itoh and S.Yoshikawa, the paper submitted to Nucl. Fusion.
2) J.I.P.P. T-II Group, IPPJ-205 (1974)
3) B.Coppi, G.Lampis and F.Pegoraro, Phys. Letters 59A (1976) 118
4) M.N.Rosenbluth and P.J.Catto, Nucl. Fusion 15 (1975) 573
5) N.T.Gladd and W.H.Horton, Phys. Fluids 16 (1973) 879
6) M.N.Rosenbluth and C.S.Liu, Phys. Fluids 15 (1972) 1801
7) S.Inoue, K.Itoh and T.Tange, IPPJ-308 (1977)
8) T.Hatori and Y.Terashima, J. Phys. Soc. Japan 42 (1977) 1010

9) W.W.Lee and H.Okuda, Phys. Rev. Letters 36 (1976) 870

10) T.Hatori, Y.C.Lee and T.Tange, J. Phys. Soc. Japan 43 (1977) 655

11) See, for example, D.F.Düchs, D.E.Post and P.H.Rutherford, Nucl. Fusion 17 (1977) 565

12) K.Matsuoka, K.Miyamoto, K.Ohasa and M.Wakatani, Nucl. Fusion, to be publishied.

13) S.Inoue, K.Itoh and S.Yoshikawa, IPPJ-302, 303 (1977)

## Appendix

We present the treatment of the electro-static current-driven drift wave in a sheared magnetic field, where the effects of both the electron and the ion temperature gradients are included, but the contribution of the trapped particles is neglected. The treatment is an extension of the previous works.[13)]

The geormetry we use is a slab and x-axis is taken in the direction both of the density gradient, $\nabla n = -\kappa n\hat{x}$, and the temperature gradient, $\nabla T = -\kappa_T T\,\hat{x}$. The magnetic field is given as $\vec{B}=(0,\ x/L_s,\ 1)B$, where the plane x=0 corresponds to the rational surface and $L_s$ is the shear length. The potential perturbation is written as $\phi(\vec{x},t) =\phi(x)\exp[iky-i\omega t]$. The longitudinal current is carried by electrons, so that we use the relation J = -neu. In the following, subscripts i and e denote ion and electron, respectively. $m_j$ and $v_j = (T_j/m_j)^{1/2}$ are the mass and the thermal speed, $\tau = T_e/T_i$. We consider the strong shear case, $1 < \kappa L_s << m_i/m_e$. As equilibrium distribution functions we use

$$f_{0j}= \frac{N_0}{(2\pi v_j^{\,2})^{3/2}}\, e^{-[\frac{v_\perp^{\,2}+(v_z-u)^2}{2v_j^{\,2}} +\kappa_j(x+v_y/\Omega_j)(1+\eta_j\frac{v_\perp^2+(v_z-u)^2}{2v_j^{\,2}} - \frac{3}{2}\eta_j)]} \tag{A-1}$$

where $v_\perp^{\,2}= v_x^{\,2}+ v_y^{\,2}$, $\eta_j = \kappa_T/\kappa$, $v_j^{\,2}(x) = T_j(x)/m_j$. For the ions we set u=0.

The basic equation for the current-driven universal drift mode is written in the dimensionless form as

$$\frac{\partial^2\phi}{\partial\zeta^2} + [\ \lambda + \mu^2\zeta^2 + \eta(\zeta)\ ]\phi = 0 \quad , \tag{A-2}$$

$$\zeta = x/\tilde{\rho}_i \ , \ \tilde{\rho}_i{}^2 = -\Lambda'\rho_i{}^2 , \ \mu^2 = \left|\frac{kv_i\tilde{\rho}_i}{L_s\omega}\right|^2 \frac{\alpha+\omega_{*T}\Lambda'}{\alpha'} \ ,$$

$$\alpha = (\tau\omega+\omega_*)\Lambda + \omega_{*T}(b\Lambda') , \quad \lambda = \frac{\alpha\Lambda' - (1+\tau)\omega\Lambda'}{\alpha'} \ ,$$

$$\eta(\zeta) = -\frac{\omega\Lambda'}{\alpha'}\left(\frac{\tilde{n}_e T_e}{n_0 e\phi} - 1\right) , \quad \Lambda = I_0(b)e^{-b} \ ,$$

where $\omega_* = k\kappa T_e/eB$, $\omega_{*T} = \eta_i\omega_*$, $\rho_i$ is the ion Larmour radius, $I_0$ is the zeroth order modified Bessel function and ' denotes the derivative with respect to b. Note that $\mu^2$ can become negative. The real frequency is given by $\lambda = 0$, that is

$$\omega = \frac{\Lambda\omega_* + b\Lambda'\omega_{*T}}{1 + \tau - \tau\Lambda} \tag{A-3}$$

We neglect the secondary (de)stabilizing effect by the real frequency shift. Figure A-1 illustrates the region in the b-$\eta_i$ plane, where $\omega < 0$ and $\mu^2 < 0$ hold. In the regions B and D, $\omega < 0$, and $\mu^2 < 0$ in the regions C and D.

Firstly, we analyze the mode whose eigen function is propagating type ($\mu^2 > 0$) and show that this mode, which is generally considered to be stable in the presence of the fairly steep electron temperature gradient[5], becomes unstable because of the longitudinal current.

To solve eq.(A-2) with eq.(A-3), we use the complete ortho-normal set $\{\phi_n\}$ with the boundary conditions for the wave to be out-going and to be regular at x=0. We express the potential perturbation as $\phi(\zeta) = \Sigma a_n\phi_n(\zeta)$,

$$\phi_n(\zeta) = \left(\frac{i\mu}{\pi}\right)^{1/4} \frac{1}{\sqrt{n!}} H_n\left(\sqrt{2i\mu}\zeta\right) e^{-i\mu\zeta^2/2} , \qquad \text{(A-4)}$$

where $H_n$ is Hermite function and $\phi_n$ satisfies the differential equation

$$\left[\frac{\partial^2}{\partial\zeta^2} + \mu^2\zeta^2 + \lambda_n\right] \phi_n = 0, \quad \lambda_n = i\mu(2n+1). \qquad \text{(A-5)}$$

Multiplying $\phi_m$ from the left side of eq.(A-2), and integrating over $\zeta$, we rewrite it into a secular equation,

$$\sum_n V_{mn} a_n = (\lambda_m - \lambda)\, a_m \qquad (m = 1,2, \cdots) \qquad \text{(A-6)}$$

$$V_{mn} = \int_{-\infty}^{+\infty} \phi_m(\zeta)\eta(\zeta)\phi_n(\zeta)d\zeta$$

In order to solve the above equation, we introduce a smallness parameter, $\varepsilon \equiv \sqrt{\mu}\zeta_e$,[4] to truncate it. For a system with the fairly strong shear, $\varepsilon$ is of the order of $\sqrt{\kappa L_s m_e/m_i}$, we retain the terms of the lowest order in $\varepsilon$. The fact that the high m modes are strongly damped ($\lambda_m \propto 2m+1$) confirms this truncation. If we let $\eta_i = \eta_e = u = 0$, and demand Im $\lambda$=0, we obtain the critical shear for the universal mode given in Ref.[4]. On the other hand for system with the current, as remarked in Ref.[6], $\eta(\zeta)$ has essentially asymmetrizing effect on $\phi$ with respect to $\zeta$. In order to include this effect, we take $(a_0, a_1)$ set and solve eq.(A-6) in 2 x 2 truncated matrix form. Even in the presence of the current and temperature gradients ($u$, $\eta_e$, $\eta_i$=0), $\varepsilon << 1$ holds. As another smallness parameter we take $u/v_e$ and retain terms in $V_{mn}$ up to the 2nd order of $u/v_e$. If we limit ourselves to the case where $\eta_i = \eta_e = 0$ and

$\omega = \omega_*$ hold, the following results recover the result in Ref.[6]. After some calculations one obtains,

$$\lambda = [(\lambda_0 - V_{00} + \lambda_1 - V_{11}) \pm \sqrt{(\lambda_0 - V_{00} - \lambda_1 + V_{11})^2 + 4V_{10}^2}]/2, \qquad \text{(A-7)}$$

$$V_{00} = i \frac{(\omega_* - \omega - \omega_* \eta_e/2)\Lambda'}{\alpha'} \sqrt{2i\varepsilon} K_0(\sqrt{2i\varepsilon}) \qquad \text{(A-8.1)}$$

$$V_{11} = - \frac{(\omega_* - \omega - \omega_* \eta_e/2)\Lambda'}{\alpha'} \varepsilon^2 K_1(\sqrt{2i\varepsilon}) \quad , \qquad \text{(A-8.2)}$$

$$V_{01} = V_{10} = i \frac{\omega \Lambda' u}{\alpha' v_e} \sqrt{2i\varepsilon} K_1(\sqrt{2i\varepsilon}) \quad , \qquad \text{(A-8.3)}$$

The growth rate $\gamma$ is given by $-\mathrm{Im}\lambda\alpha'/\Lambda'(1+\tau-\tau\Lambda)$. The condition Im $\lambda=0$ gives the equation for the critical shear stabilization condition,

$$6\mu^3 + 5\varepsilon \ln\frac{\sqrt{2}}{\varepsilon} \frac{(\omega_* - \omega - \omega_* \eta_e/2)}{\alpha'} \mu^2 - 2\left(\frac{\omega \Lambda' u}{\alpha' v_e}\right)^2 \mu \geqq 0 \ . \qquad \text{(A-9)}$$

To obtain this, we don't treat the $\eta(\zeta)$ term in eq.(A-2) as a perturbation from the rest. Products of two expanding parameters $\varepsilon$ and $u^2/v_e^2$ and higher order terms are neglected. When we consider the case where $u/v_e=0$ with fairly steep electron temperature gradient, we see from eq.(A-9), that the mode is stable even in the shearless field. However, if there is a force free current in the plasma, $\eta_e$ alone is insufficient to stabilize the current-driven (CD) mode, and the concept of the critical shear becomes important. From eq.(A-9) we find that even in the presence of $\eta_e > 0$, the mode becomes unstable unless the shear is sufficient. Because the instability source of the CD mode, $k_{\parallel}u$ (=kux/$L_s$), is proportional to the shear

strength, the growth rate of this instability is affected not directly by the convective damping but by the localizing effect of the shear. We note that the instability driving term due to the current is insensitive to the shear.

Another important fact is the ion temperature gradient effect on the CD mode. One effect is as follows. The value $\mu$ becomes small as $\eta_i$ increases ; the ion temperature gradient tends to reduce the shear stabilization effect. As $\mu$ decreases, the convective damping decreases faster than the wave localization effect. So that as $\eta_i$ increases the current destabilizing term remains large in comparison with other terms in eq.(A-9). Another effect of $\eta_i$ is that the real frequency decreases and even becomes negative as indicated by eq.(A-3). The value of $\eta_i$ to change the sign of $\omega$, $\eta_0$, is also plotted in Fig.A-1. In the region B where $\mu^2 > 0$ and $\eta_i > \eta_0$ hold, the electron temperature gradient becomes destabilizing source. The sign of the second term of eq.(A-9) changes and the critical shear condition becomes harder.

In the above arguments we study the case of $\mu^2 > 0$. As $\eta_i$ increases to exceed the critical value $\eta_c$, $\mu^2 < 0$ holds and the convective damping by the shear is annihilated. The effect of the shear turns out only to determine the wave localization width. The method to analyze this mode is almost the same as discussed before. The difference is that the term $i\mu$ is replaced by $\mu$ (or $-\mu$). As the boundary condition we demand the wave vanishes as $|x| \to \infty$. The eigen function of this evanescent type gives rise to a real frequency shift

instead of the convective damping. The critical shear is given by the same condition Im $\lambda$=0. In the region D of Fig.A-1 the critical shear is given by $|\mu| \geq |\omega\Lambda' u/\sqrt{3}v_e\alpha'|$. In D the mode is stable in the absence of u. In region C in Fig.A-1, where the mode is unstable even if u=0, the shear stabilization may be impossible. We see that the current driven mode is insensitive to the convective damping, because the driving term becomes greater as the shear increases.

Finally we estimate the ratio of the pressure fluctuation ($\tilde{p}/p = \frac{m}{3}\int v^2\tilde{f}\, d^3v/p$) and the density fluctuation ($\tilde{n}/n = \int \tilde{f}\, d^3v/n$). In the sheared magnetic field, these fluctuations have profiles around the rational surface. The profiles of $\tilde{n}/n$ normalized to $e\phi/T_e$ and $(\tilde{p}/p)/(\tilde{n}/n)$ are shown in Fig.(A-2) as functions of the distance from the rational surface. When we compare the peak values of the fluctuations, we find

$$(\tilde{p}/p)/(\tilde{n}/n) = (1 + \eta_e) \quad . \qquad \text{(A-10)}$$

The contribution from the current to the fluctuation levels is small, although its contribution to the particle and heat fluxes is larnge.

Our result about the $\eta_i$ effect, destabilizing when $\eta_i > 0$, is opposed to the numerical calculation in Ref.[5]. This is because the ion temperature effect is misincluded in the basic equation of Ref.[5].

When the value of $\eta_i$ is very close to the values $\eta_0$ and/or $\eta_c$, our analysis is inapplicable because $d/d\zeta$ term or higher order derivative terms are no longer negligibly small in

deriving eq.(A-12). When $\eta_i$ becomes fairly large, the ion branch which is not analyzed here may become of importance.

## Figure Captions

Fig.1 Slab model

Fig.2 The energy confinement time $\tau_E$ is given as a function of the averaged density. The transport in the lower density region is determined by the current-driven instability, while in the higher density region the ordinary collisional drift instability is responsible for it. The expected experimental conditions in J.I.P.P. T-II device are also indicated.

Fig.3 $u/v_e$ is the electron current velocity divided by its thermal speed and $1/\kappa L_s$ is the scale of the density gradient divided by the shear length. Both the quantities are plotted as a function of r/a for two values of $\eta_e = \nabla \ln T_e / \nabla \ln n$, assuming the radial distributions in Table 3.

Fig.4 The radial dependence of the diffusion coefficient D for the different values of the averaged density $\bar{n}$.

Fig.5 The dependence of the diffusion coeffecient on the density n for the different positions in the radial direction.

Fig.6 Schematic diagram of the instability criteria in $(r, \bar{n})$ space. The shaded portion for each $\eta_e$ is the region, divided by the solid line $\nu_{eff}/\omega_b = 0.5$, where the dissipative trapped electron instability may appear. The dotted lines show the condition of $\nu_{eff}/\omega_b = 1$. The chained lines show the condition of $u/v_e = 1/\kappa L_s$. The expected experimental conditions in

J.I.P.P. T-II device are also indicated.

Fig.7 Two typical experimental procedures by superposing the helical magnetic field in J.I.P.P. T-II device.

Fig.A-1 The b - $\eta_i$ plane divided into 4 regions. In the regions B and D, $\omega < 0$ holds. In the regions C and D, $\mu^2$ is negative and the convective damping of the wave is annihilated.

Fig.A-2 The levels of the perturbation in the vicinity of the rational surface at $r = r_s$. The line 1 shows the density perturbation normalized to $e\phi/T_e$, and the line 2 shows the ratio $(\tilde{p}/p)/(\tilde{n}/n)$.

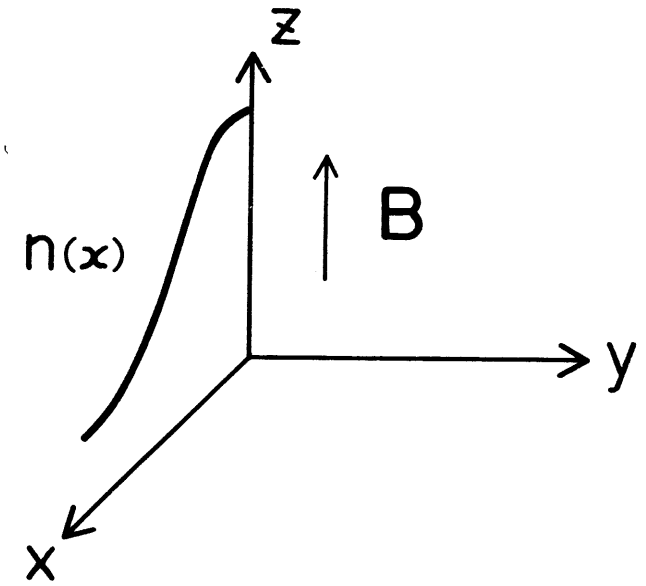


Fig. 1

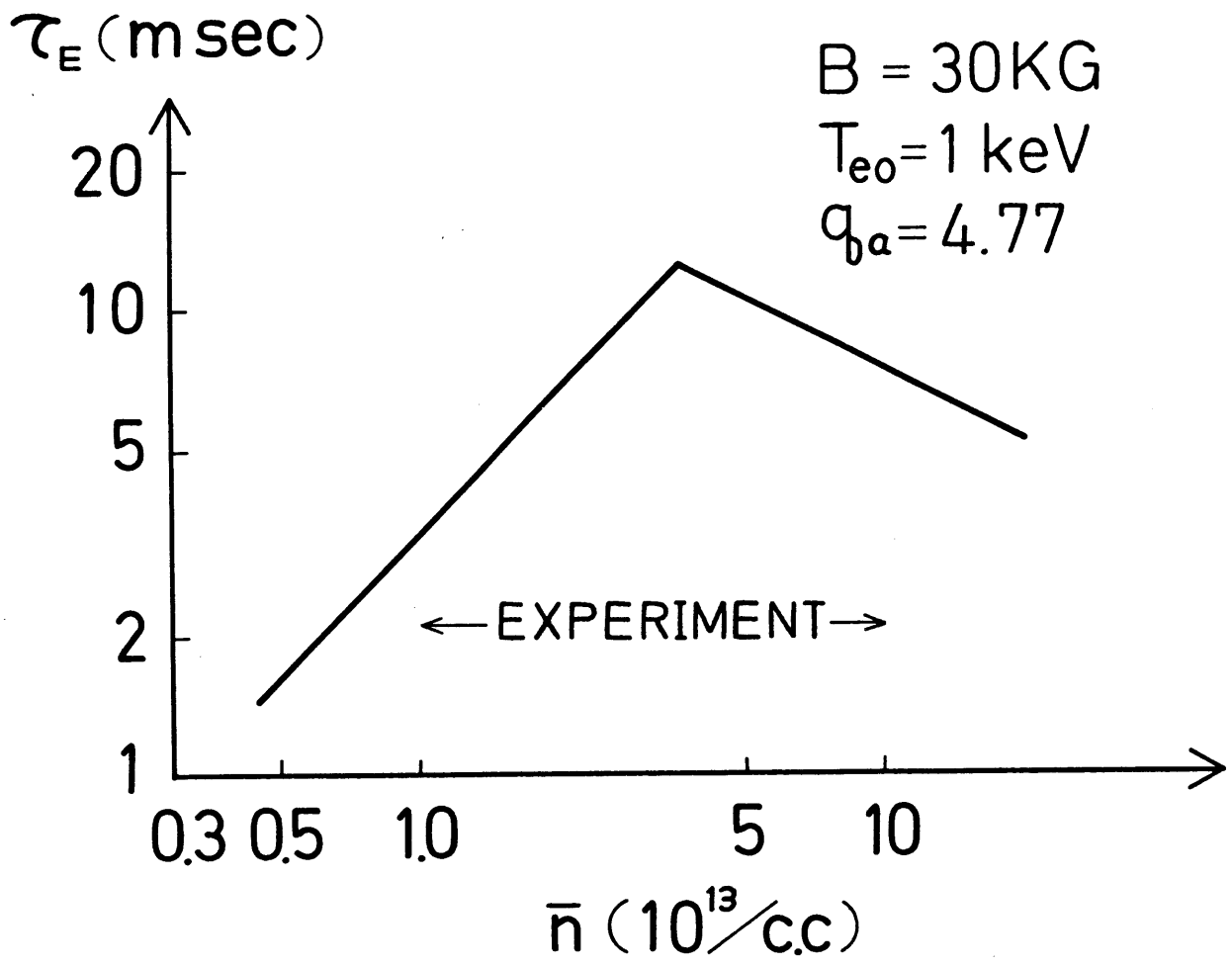
$\tau_E$ (m sec)
B = 30KG
$T_{eo}$ = 1 keV
$q_{ba}$ = 4.77
20
10
5
2
1
← EXPERIMENT →
0.3 0.5 1.0 5 10
$\bar{n}$ ($10^{13}$/c.c)

Fig. 2

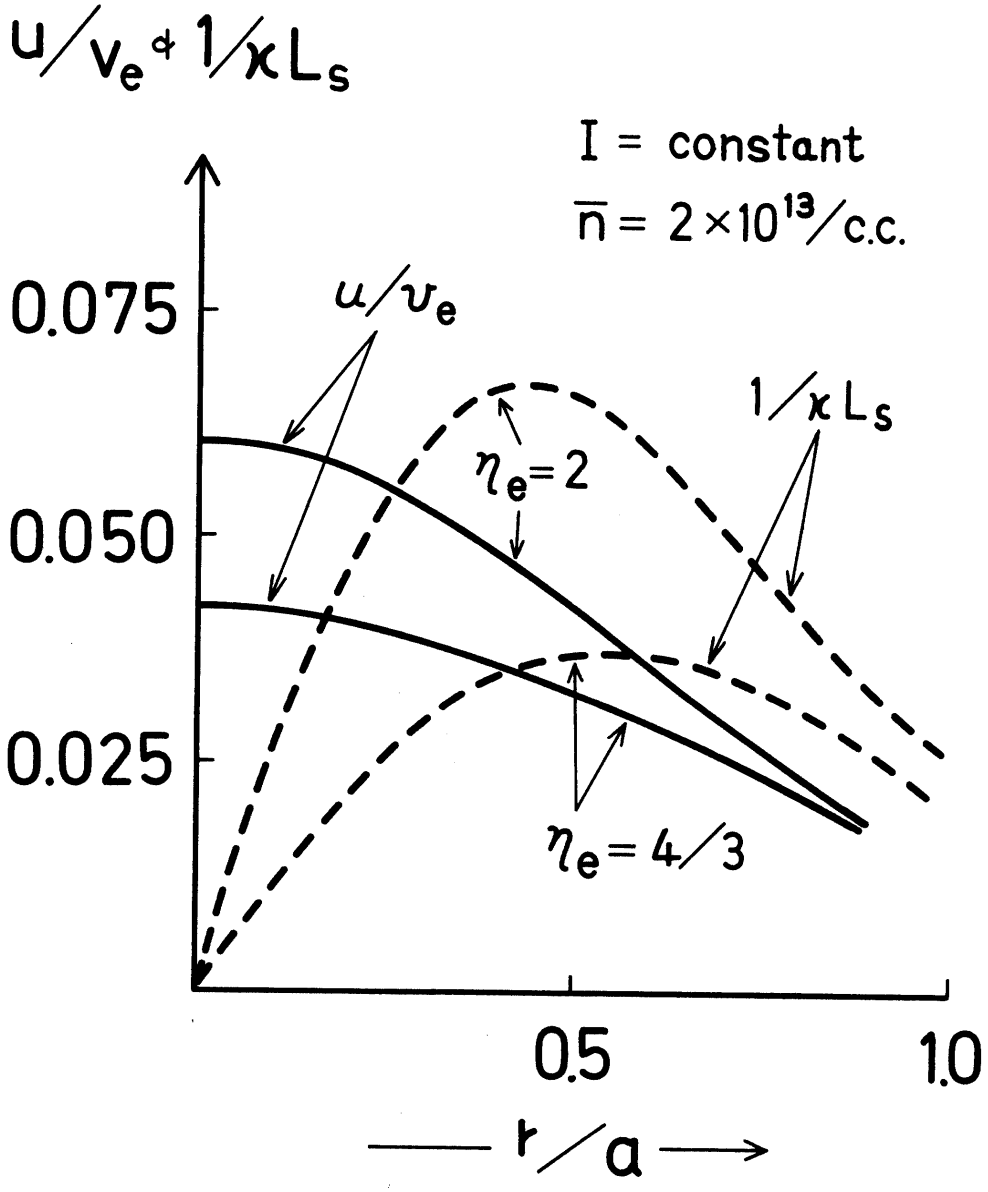
u/v_e & 1/κL_s
I = constant
n̄ = 2×10^13/c.c.
0.075
0.050
0.025
u/v_e
1/κL_s
η_e = 2
η_e = 4/3
0.5
1.0
r/a

Fig. 3

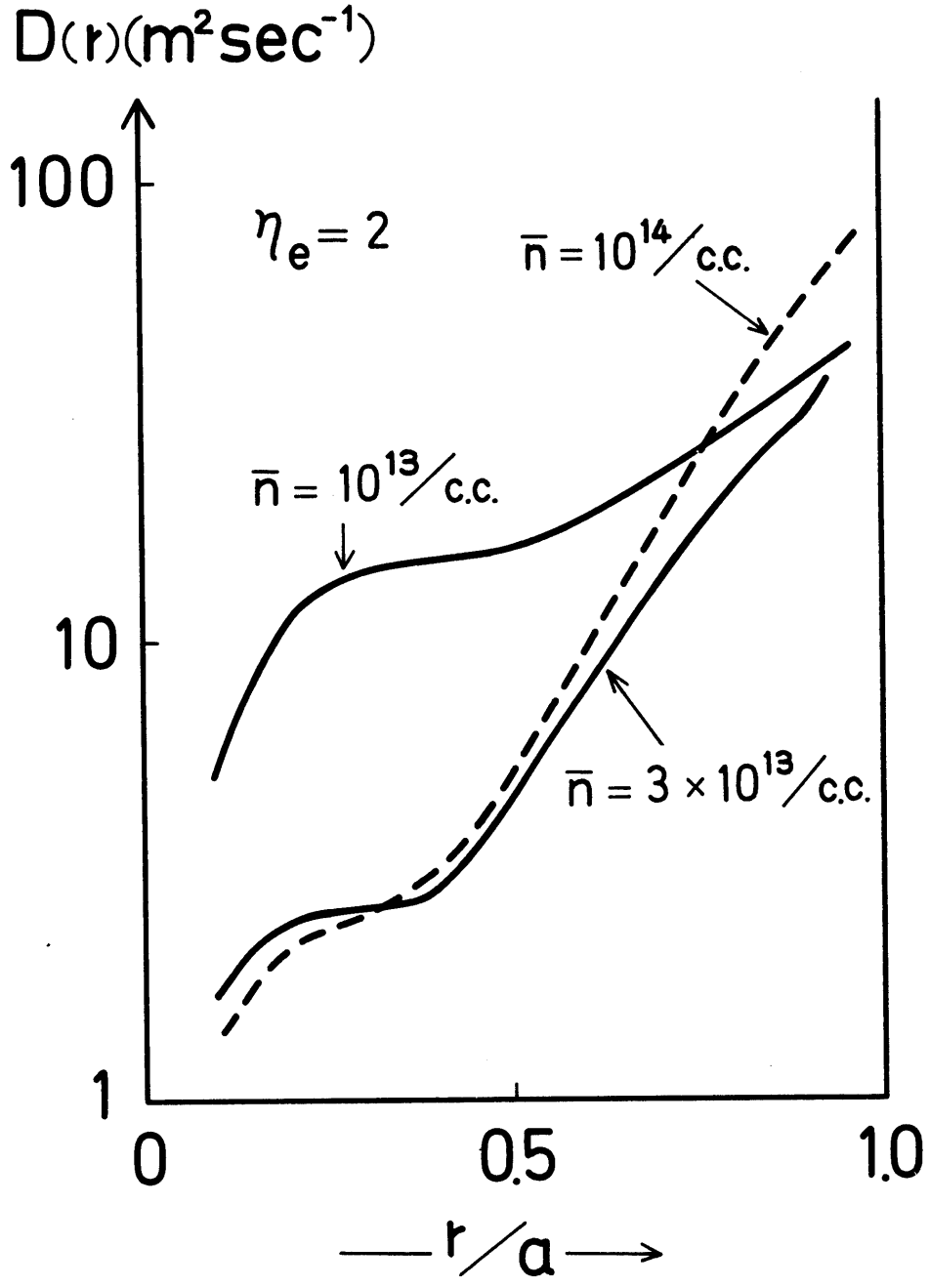
D(r)(m²sec⁻¹)
100
10
1
$\eta_e = 2$
$\bar{n} = 10^{14}$/c.c.
$\bar{n} = 10^{13}$/c.c.
$\bar{n} = 3 \times 10^{13}$/c.c.
0
0.5
1.0
r/a

Fig. 4

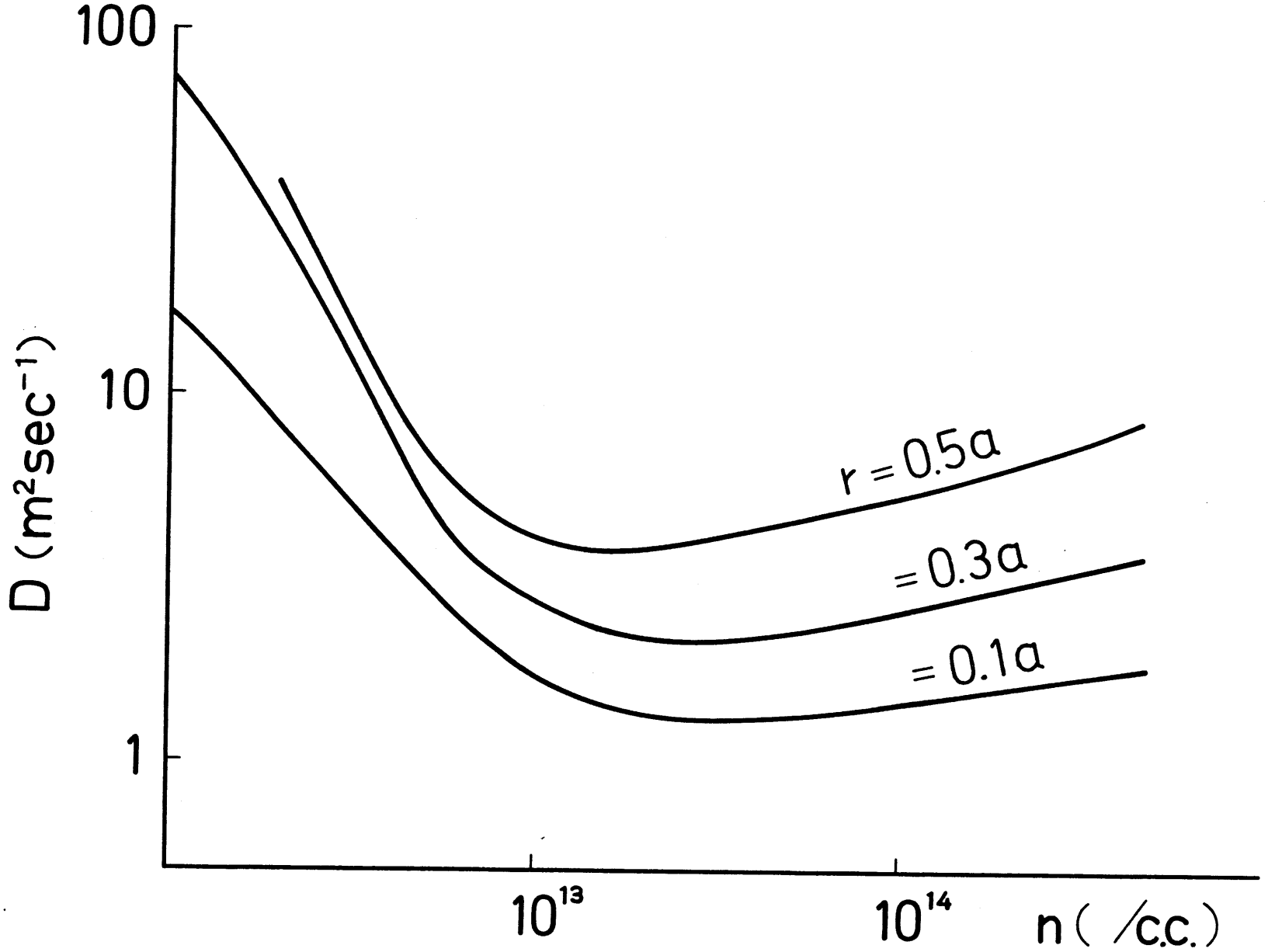


Fig. 5

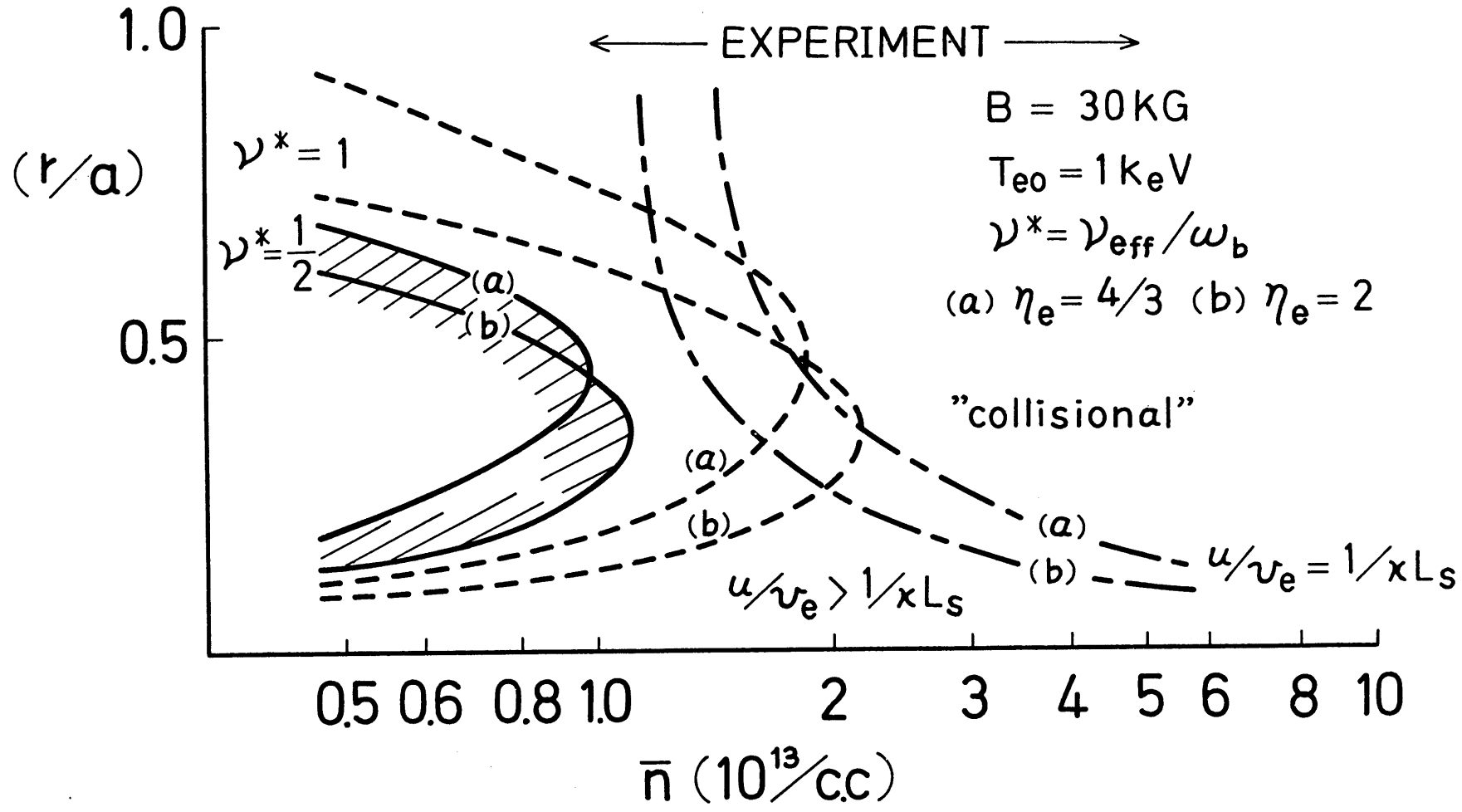
1.0
0.5
(r/a)
← EXPERIMENT →
B = 30KG
Teo = 1keV
ν* = νeff/ωb
(a) ηe = 4/3 (b) ηe = 2
ν* = 1
ν* = 1/2
(a)
(b)
"collisional"
(a)
(b)
u/ve > 1/xLs
(a)
(b)
u/ve = 1/xLs
0.5 0.6 0.8 1.0 2 3 4 5 6 8 10
n̄ (10¹³/c.c)

Fig. 6 ,

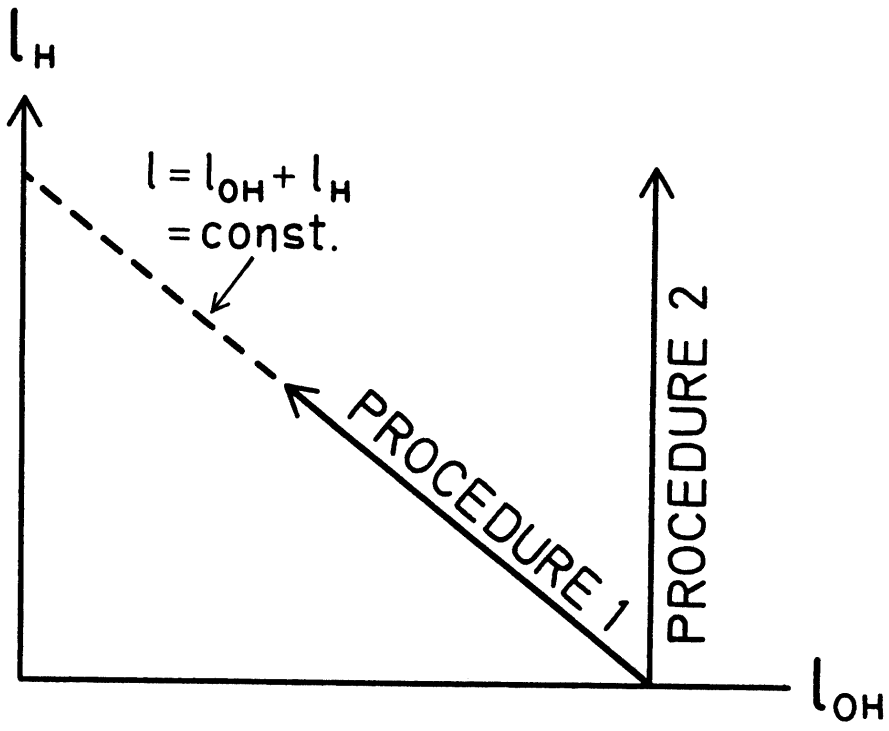


Fig. 7

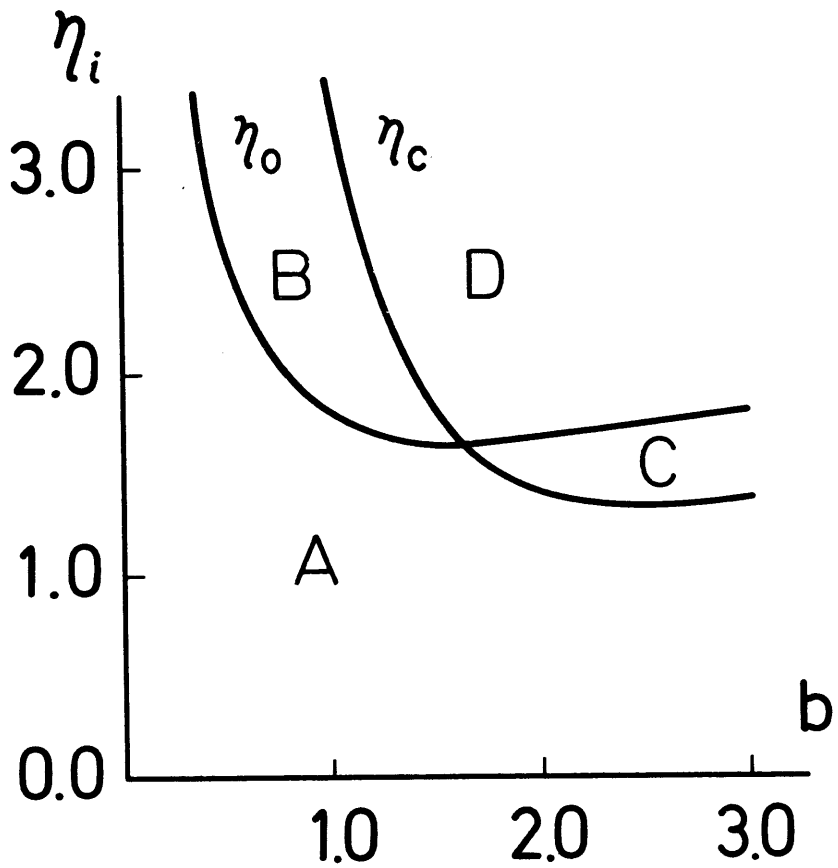


Fig. A 1

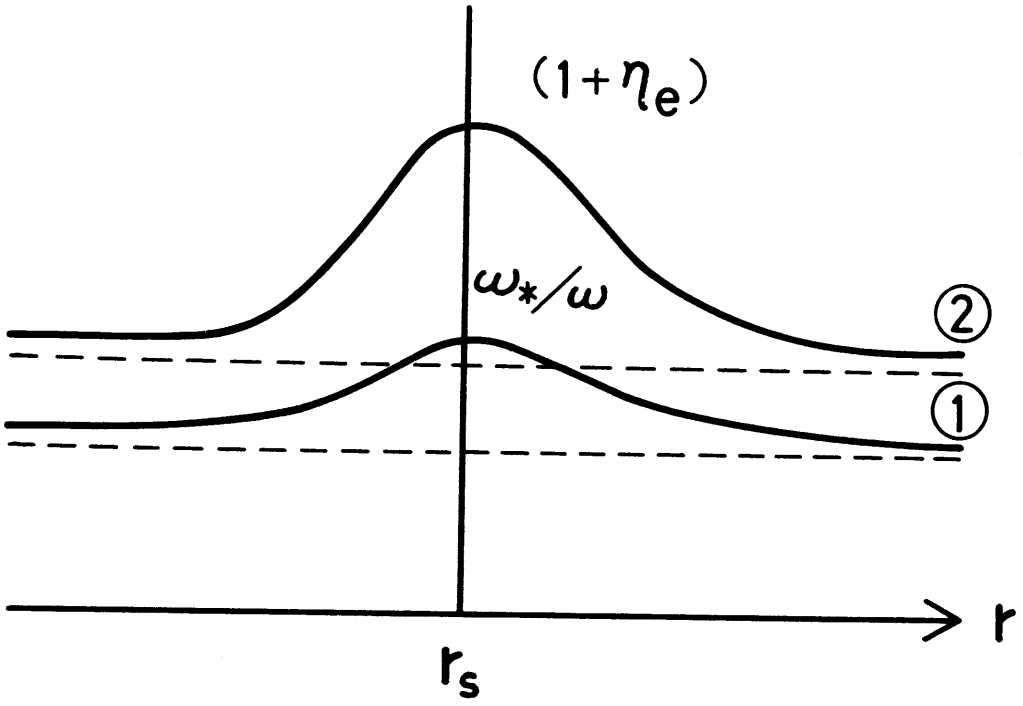


Fig. A 2